Controlled synthesis of size-tunable nickel and nickel oxide nanoparticles using water-in-oil microemulsions

OPEN ACCESS
IOP PUBLISHING
ADVANCES IN NATURAL SCIENCES: NANOSCIENCE AND NANOTECHNOLOGY
Adv. Nat. Sci.: Nanosci. Nanotechnol. **4** (2013) 025009 (9pp)
doi:10.1088/2043-6262/4/2/025009

Controlled synthesis of size-tunable nickel and nickel oxide nanoparticles using water-in-oil microemulsions

Ajeet Kumar[1], **Amit Saxena**[1], **Arnab De**[2], **Ravi Shankar**[1] **and Subho Mozumdar**[1]

[1] Department of Chemistry, University of Delhi, Delhi 110007, India
[2] Department of Microbiology and Immunology, Columbia University, USA

E-mail: subhoscom@yahoo.co.in

Received 11 November 2012
Accepted for publication 3 April 2013
Published 19 April 2013
Online at stacks.iop.org/ANSN/4/025009

Abstract
Industrial demands have generated a growing need to synthesize pure metal and metal–oxide nanoparticles of a desired size. We report a novel and convenient method for the synthesis of spherical, size tunable, well dispersed, stable nickel and nickel oxide nanoparticles by reduction of nickel nitrate at room temperature in a TX-100/*n*-hexanol/cyclohexane/water system by a reverse microemulsion route. We determined that reduction with alkaline sodium borohydrate in nitrogen atmosphere leads to the formation of nickel nanoparticles, while the use of hydrazine hydrate in aerobic conditions leads to the formation of nickel oxide nanoparticles. The influence of several reaction parameters on the size of nickel and nickel oxide nanoparticles were evaluated in detail. It was found that the size can be easily controlled either by changing the molar ratio of water to surfactant or by simply altering the concentration of the reducing agent. The morphology and structure of the nanoparticles were characterized by quasi-elastic light scattering (QELS), transmission electron microscopy (TEM), x-ray diffraction (XRD), electron diffraction analysis (EDA) and energy dispersive x-ray (EDX) spectroscopy. The results show that synthesized nanoparticles are of high purity and have an average size distribution of 5–100 nm. The nanoparticles prepared by our simple methodology have been successfully used for catalyzing various chemical reactions.

Keywords: nickel nanoparticles, nickel oxide nanoparticles, water-in-oil microemulsions, non-ionic surfactant

Classification number: 4.02

1. Introduction

Nanoparticles in general have different electronic, magnetic and chemical properties as compared to the property of the bulk material. The main reason for that is their large surface-to-volume ratio which results from their small sizes. Nickel nanoparticles in particular have been used in chemical cells, fuel cells, for solar energy absorption, as catalysts [1], as magnetic materials, etc [2, 3]. Nickel nanoparticles when mixed in minima amounts (1%) with solid rocket propellant can double its heat of combustion [4]. The demand for nano-nickel material has risen with the rapid development of different telecommunication equipments [5]. Therefore, it is necessary to develop a protocol for synthesizing well dispersed, stable, nickel nanoparticles with different sizes so as to meet different demands. The protocol will be most useful if the sizes of the synthesized particles can be tuned by adjusting simple reaction parameters.

There are a number of ways to synthesize nickel nanoparticles, however, they all suffer from crucial shortcomings. These methods include chemical vapor deposition (CVD) [6], wet chemical [4, 7], laser-driven

aerosol [8], hydrothermal [9], co-precipitation [10], sol–gel [11] and microemulsion [12–14]. However, the reported methodology is not always convenient for the production of monodispersed, stable and ultra-low sized nanoparticles as it requires extensive use of expensive equipment and difficult production conditions. Typically, preparation of nickel involves the solution phase chemistry route, which in theory should provide multiple, simple ways to control the morphology, particle size and desirable crystalline phase. Ideally, the process should be amenable to scaling up. Nickel nanoparticles have been synthesized by reduction of metal salts using reducing agents such as $NaBH_4$ [15, 16], hydrazine [17–20] and polyols [21–25]. While these processes can produce spherical, stable nanoparticles without agglomeration; the synthesized particle surfaces are often found to be rough and exhibit spiky surface morphology [26–28].

Water-in-oil (w/o) microemulsion solutions can serve as a model medium for synthesis of very fine and monodispersed [29–31] nanoparticles. Firstly, they can act as microreactors for the reaction. Additionally, they can inhibit agglomeration of the particles as there is a self-correcting tendency of the surfactants adsorbing on the particle surface if the particle size approaches that of the water pool.

We disclose herein a method for the synthesis of well dispersed, sphere-shaped, highly stable nickel and nickel oxide nanoparticles in similar microemulsion pool. We discover that the use of alkaline sodium borohydrate in nitrogen atmosphere leads to the formation of nickel nanoparticles, while the use of hydrazine hydrate in aerobic conditions leads to the formation of nickel oxide nanoparticles. Additionally, the size of the nickel and nickel oxide nanoparticles can be easily controlled either by changing the molar ratio of water to surfactant or by altering the concentration of the reducing agent W_o. The protective nature of the surfactant molecules prevents the nanoparticles from oxidation (in the case of metallic nickel nanoparticles) and agglomeration. The method does not require elevated temperature and the entire synthesis can be carried out at room temperature.

2. Material and methods

All the experiments were performed at room temperature. Electron micrographs were taken with a TEM TECHNAI 300 kV, Ultra twin FEI with EDAX transmission electron microscope operating at 300 kV. The average particle diameter of the prepared nanoparticles was carried out by a dynamic light scattering instrument (Photocor FC, USA). The measuring range was from 1 to 5000 nm and the light source was He–Ne 633 nm laser diode of 1–40 MW. Data analysis was performed with Alango Dynal V 2.0 Software. Wide angle x-ray diffraction pattern was obtained for nickel and nickel oxide nanoparticles by using a Philips analytica PW 1830 x-ray VB equipped with a 2θ compensating slit, CuK_α radiation (1.54 Å) at 40 kV, 40 mA passing through Ni filter with a wavelength of 0.154 nm at 20 mA and 35 kV. Data collection was made in a continuous scan mode with a step size of 0.01° and step time of 1 s over a 2θ range of 30–90°. Data analysis was performed with PC-APD diffraction software.

2.1. Preparation of nickel and nickel oxide nanoparticles

A typical synthesis of the nickel nanoparticles involved the mixing of two reverse microemulsions (RM-A and RM-B). RM-A was prepared by taking 25 ml of 0.1 M solution of TX-100 in cyclohexane and adding 300 μl of *n*-hexanol and 225 μl of a 5% (w/v) aqueous solution of $Ni(NO_3)_2$. Similarly, RM-B was prepared by taking 25 ml of 0.1 M solution of TX-100 in cyclohexane and adding 300 μl of *n*-hexanol and 225 μl of a 5% (w/v) aqueous solution of alkaline $NaBH_4$. The typical W_o value of this system was found to be 5. Both the microemulsions were left stirring for 30 min to obtain an optically clear homogeneous dispersion. RM-B was then added to RM-A in a drop-wise manner with continuous stirring. The resulting solution was left stirring for another 3 h to allow complete particle growth via Ostwald ripening. Instant appearance of black color indicates the formation of nickel nanoparticles. Nitrogen atmosphere was maintained throughout the reaction procedure to ensure the complete removal of oxygen. For the synthesis of nickel oxide nanoparticles, amount and concentration of the reactants were similar to that of nickel nanoparticles. However, the reduction reaction was carried out using 5% (w/v) $N_2H_4 \cdot H_2O$ solution in an aerobic condition instead of alkaline $NaBH_4$ in a nitrogen atmosphere. A diagrammatic scheme for the preparation of nickel and nickel oxide nanoparticles using reverse microemulsion is shown in scheme 1.

3. Results and discussion

The nucleation step and the growth step are the two major steps in the process of synthesizing stable nanoparticles [32, 33]. It is conceivable that one could change the reaction parameters as a way of controlling these two crucial steps. Aqueous core of the reverse micellar solution behaves as a tiny reaction vessel which was exploited for the reaction of nickel nitrate with alkaline sodium borohydride under nitrogen atmosphere so as to generate highly stable, black colored, optically clear solution of nickel nanoparticles. However, when hydrazine hydrate is used as a reducing agent, the reverse micellar solution gives an off-white colored, optically clear solution of nickel oxide nanoparticles (scheme 1). It was experimentally determined that sodium borohydrate reduced $Ni(NO_3)_2$ to nickel nanoparticles; however, an inert nitrogen atmosphere is required for this (to prevent oxidation of the reduced metal). On the other hand, hydrazine hydrate reduced $Ni(NO_3)_2$ to nickel oxide nanoparticles in an aerobic condition. Various other reaction parameters were studied to tailor the size and morphology of the nanoparticles as needed.

3.1. Influence of W_o over particle size

W_o can be defined as the ratio of molar concentration of water to surfactant. The composition of the solution has a major effect in the size of the droplet of the microemulsion. If the size of the particle approaches that of the microemulsion droplet, the surfactant molecules get adsorbed on the surface of the particle. The surfactant molecules can now act as a protective agent. Thus, the composition of the microemulsion solution influences not only the stability of microemulsion

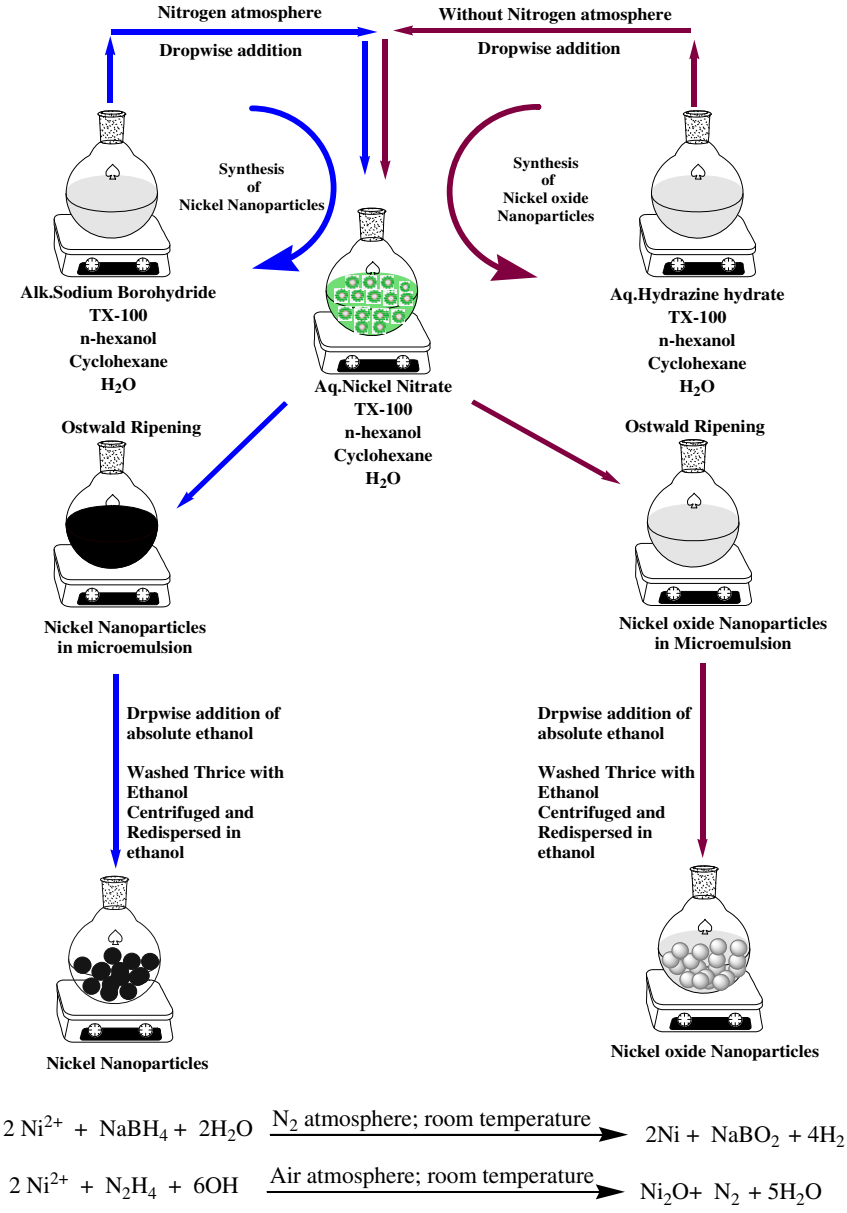

$$2\,Ni^{2+} + NaBH_4 + 2H_2O \xrightarrow{N_2\ \text{atmosphere; room temperature}} 2Ni + NaBO_2 + 4H_2$$

$$2\,Ni^{2+} + N_2H_4 + 6OH \xrightarrow{\text{Air atmosphere; room temperature}} Ni_2O + N_2 + 5H_2O$$

Scheme 1. General procedure for the synthesis of nickel and nickel oxide nanoparticles.

Table 1. Effect of variation of W_o on the diameter of nickel and nickel oxide nanoparticles.

W_o	Diameter of nickel nanoparticles (nm) ±2 nm	Remarks	Diameter of nickel oxide nanoparticles (nm) ±2 nm	Remarks
1	8	Precipitated in 1 h	9	Stable
3	16	Stable	13	Stable
5	29	Stable	20	Stable
7	59	Stable	39	Stable
9	68	Stable	86	Stable
11	81	Stable	110	Stable
13	–	Precipitated	–	Precipitated
15	–	Precipitated	–	Precipitated

Conditions: concentration of $Ni(NO_3)_2$ (aqueous solution (aq. sol.)) is 2% (w/v), concentration of N_2H_4 (aq. sol.) is 5% (w/v), set volume is 25 ml, surfactant concentration is 0.1 M, concentration of $NaBH_4$ (alk. sol.) is 5% (w/v), co-surfactant used *n*-hexanol.

system but also the formation and growth of the nanoparticles. The average diameters for all of the nickel nanoparticles obtained at different W_o are tabulated in table 1 and shown in figure 1. In general, the size of the nanoparticles increases with the W_o value. As shown in table 1 and figure 1, the size of the nickel particles increases from an average diameter of 8–100 nm as the W_o value increases from 1 to 11. Thus, increase of water content leads to bigger nanoparticles

Table 2. Effect of variation of reducing agent concentration on the diameter of nickel and nickel oxide nanoparticles.

Reducing agent concentration (% w/v)	Diameter of nickel nanoparticles (nm) ±2 nm	Remarks	Diameter of nickel oxide nanoparticles (nm) ±2 nm	Remarks
0.01	34	Precipitated in 20 min	43	Stable
0.05	31	Stable	40	Stable
0.10	30	Stable	38	Stable
0.50	30	Stable	38	Stable
1.00	31	Stable	39	Stable
2.00	30	Stable	38	Stable
4.00	29	Precipitated	37	Precipitated
8.00	30	Precipitated	38	Precipitated

Conditions: concentration of $Ni(NO_3)_2$ (aq. sol.) is 2% w/v, set volume is 25 ml, surfactant concentration is 0.1 M, co-surfactant used *n*-hexanol.

Table 3. Effect of variation of nickel nitrate concentration on the diameter of nickel and nickel oxide nanoparticles.

Metal ion concentration (% w/v)	Diameter of nickel nanoparticles (nm) ±2 nm	Remarks	Diameter of nickel oxide nanoparticles (nm) ±2 nm	Remarks
0.01	10	Precipitated in 20 min	11	Stable
0.05	09	Stable	41	Stable
0.10	08	Stable	08	Stable
0.50	06	Stable	08	Stable
1.00	06	Stable	07	Stable
2.00	30	Stable	27	Stable
4.00	32	Precipitated	33	Precipitated
8.00	33	Precipitated	36	Precipitated

Conditions: concentration of N_2H_4 (aq.sol.) is 5% w/v, set volume is 25 ml, surfactant concentration is 0.1 M, co-surfactant used *n*-hexanol

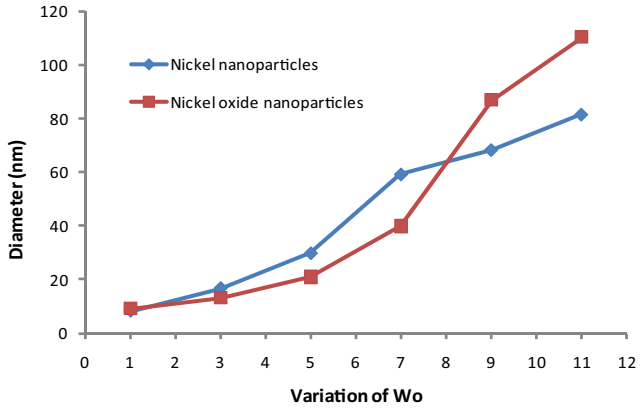

Figure 1. Effect of variation of W_o on the diameter of nickel and nickel oxide nanoparticles.

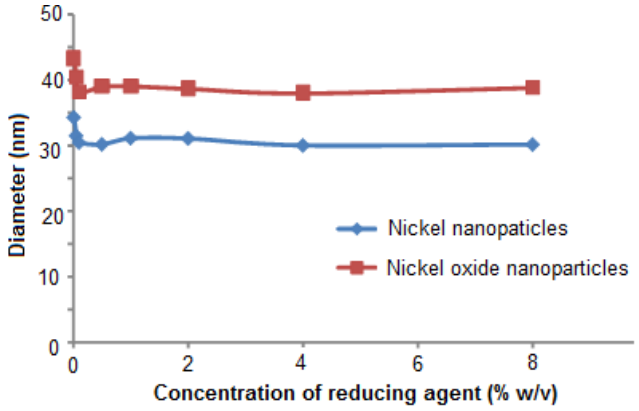

Figure 2. Effect of variation of reducing agent concentration on the diameter of nickel and nickel oxide nanoparticles.

(greater diameter). Additionally, this also shows that the particle diameter depends on the initial size of droplets of the emulsion, (microreactor effect).

With increasing W_o value, the larger water pool provides a larger space for nanoparticles to grow. This is primarily responsible for the corresponding synthesis of larger particles. No investigation was performed when the W_o was above 11 because the microemulsion solution became extremely unstable and phase separation occurred.

3.2. Effect of concentration of reducing agent on particle size

The effect of the concentration of reducing agent on the size of nickel and nickel oxide nanoparticles has also been

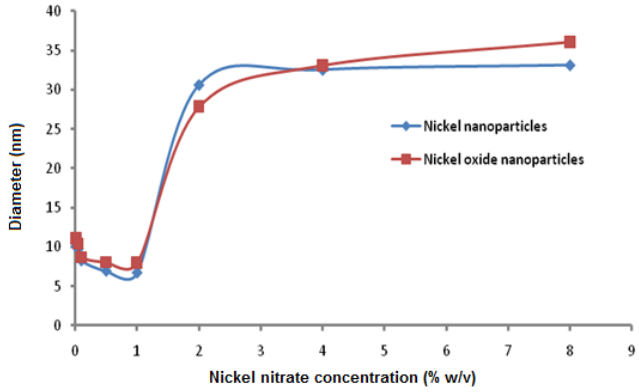

Figure 3. Effect of variation of nickel nitrate concentration on the diameter of nickel and nickel oxide nanoparticles.

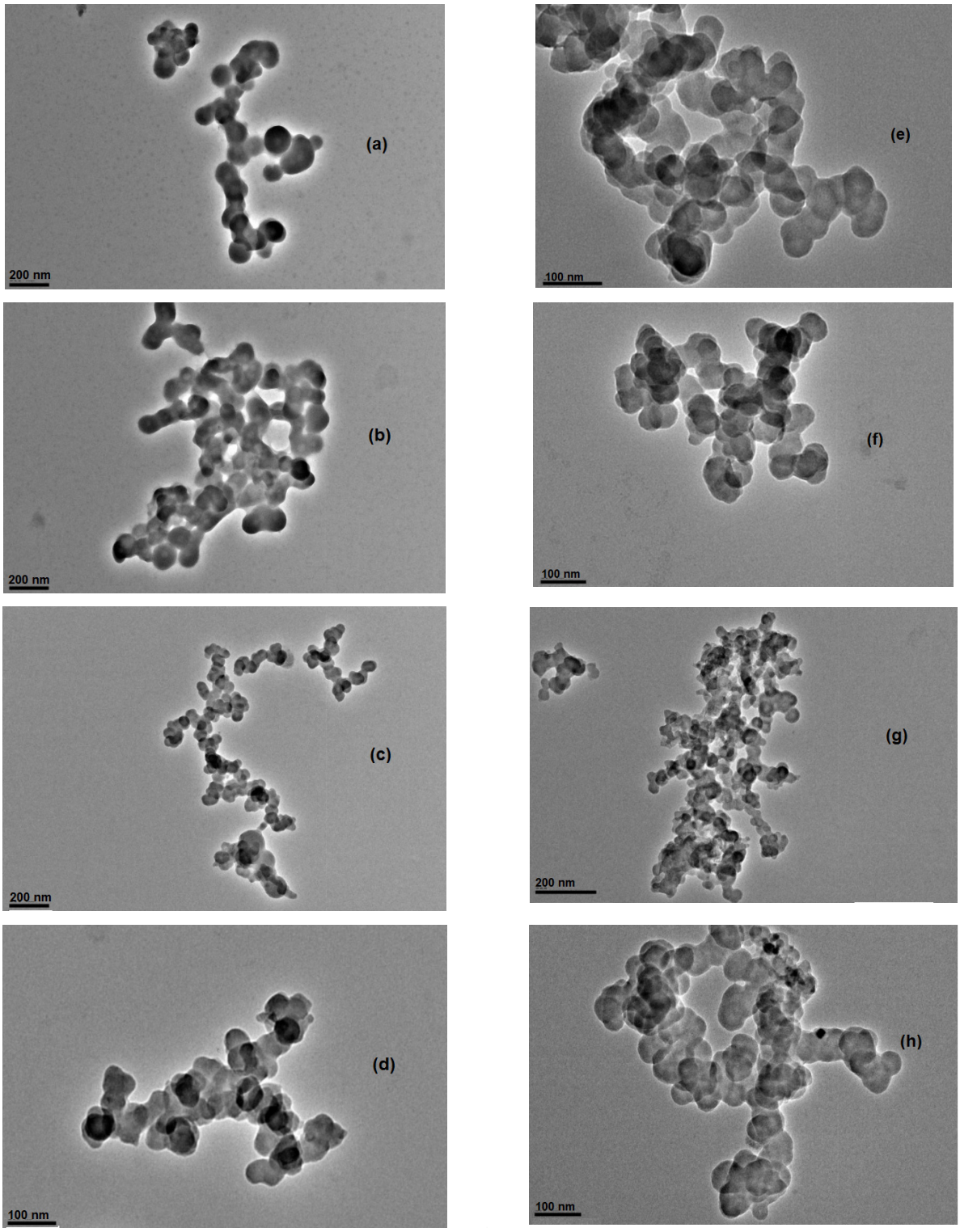

Figure 4. TEM micrograph of (a)–(d) nickel nanoparticles and (e)–(h) nickel oxide nanoparticles.

investigated in the microemulsion system of water/TX-100/cyclohexane/*n*-hexanol at a W_o value of 5, keeping the concentration of the metal ion constant at 2% w/v. The results have been tabulated in table 2 and presented in figure 2. It can be seen that the average diameters of nanoparticles decreased with the increase of the concentration of the reducing agent and before reaching a constant value.

The size and stability of nanoparticles mainly depends upon the nucleation and the subsequent growth rate to form stable nanoparticles. In the beginning, a minimal number of atoms get together to form a stable nucleus. Subsequently, collisions between these atoms lead to the assembly of stable nanoparticles. Hence, one can assume that once the nuclei are formed, the growth process supersedes the nucleation.

We observed that the nanoparticles were mono-dispersed. This was probably because the nuclei were all formed together and grew at the same rate. Hence one can conclude that it is the number of nuclei formed at the beginning of the reduction

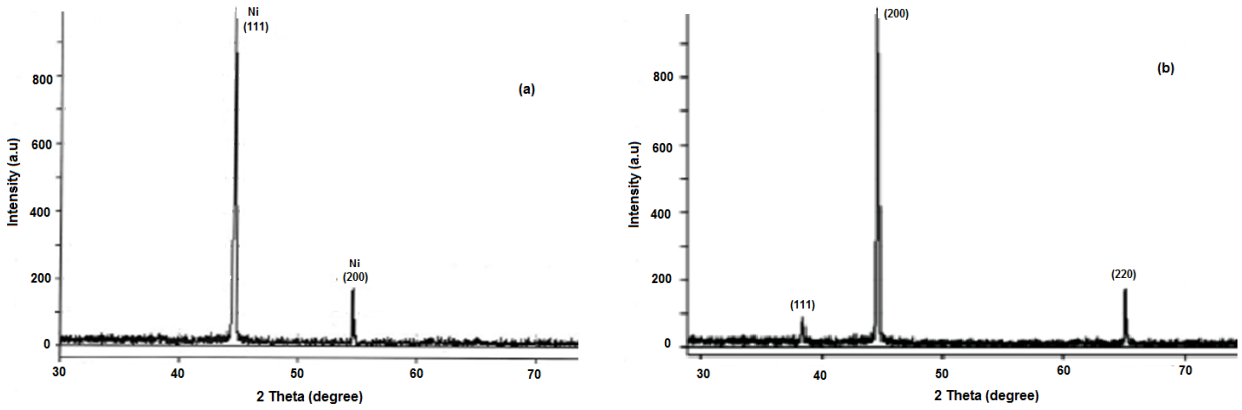

Figure 5. X-ray diffraction of (a) nickel nanoparticles and (b) nickel oxide nanoparticles.

(a) **(b)**

Figure 6. Electron diffraction of nickel nanoparticles (a) and nickel oxide nanoparticles (b).

that essentially determines the number and size of the resultant particles.

3.3. Effect of concentration of metal ion on particle size

The effect of the concentration of nickel nitrate on the size of nickel/ nickel oxide nanoparticles has also been investigated in the microemulsion system of water/TX-100/ cyclohexane/*n*-hexanol at a W_o value of 5, keeping the concentration of the reducing agent constant (2% w/v). The results are tabulated in table 3 and shown in figure 3. It can be seen that the effect of the concentration of the metal ions follows an 'S'-shaped curve. This means that on increasing the concentration of the metal ions, the average diameter of the nanoparticles so formed initially decreases, approaches a constant value and then reaches a final stabilized value.

We observed that the size of the nanoparticles did not change initially with the concentration of the metal ion. However, when the concentration of the nickel nitrate was above 1% w/v, the average diameters of nickel nanoparticles increased significantly. The initial concentration of the reducing agent was very high with respect to the metal ion concentration and this led to the formation of small and unstable nuclei. With increasing concentration of the metal ions, the number of nuclei formed at the very beginning of the reduction remained constant. The atoms formed at the latter period were used for the growth of particles. This resulted in the formation of larger and stable particles.

4. Characterization of nickel and nickel oxide nanoparticles

4.1. Transmission electron microscopic (TEM) analysis

In order to prepare the samples for TEM analysis, approximately 5 mg of the dry nanoparticles were dispersed in 25 ml of ethanol using an ultrasonicator and this yielded a clear dispersed solution of the nanoparticles. 10 μl of this nanoparticle dispersion was put on a formvar coated copper grid (1% solution of formvar was prepared in spectroscopic grade chloroform) and air-dried in a vacuum desiccator. The dried grid was then examined under an electron microscope (TEM TECHNAI 300 KV, Ultra twin FEI with EDAX transmission electron microscope operating at 300 kV).

Figures 4(a)–(d) and (e)–(h) show the TEM images of nickel nanoparticles and nickel oxide nanoparticles, respectively, at an optimized parameter. The resulting spherical nanoparticles were monodispersed and this confirms that all the nuclei were formed almost at the same time and grew at the same rate. The results obtained were analyzed and it was found that they were in accordance with the results obtained from QELS and there were no signs of agglomeration. The particles were uniform in shape and well dispersed. The particle size ranged from 8 to 100 nm.

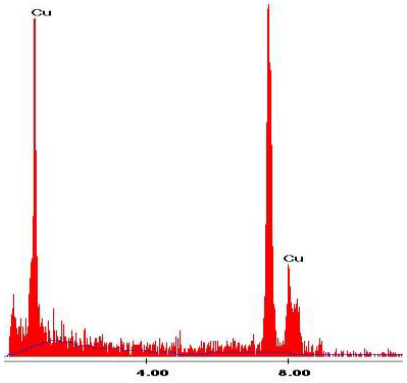

Element	Weight %	Atomic %	Net inte.	Backgrd.	Inte. error	P/B
NiK	80.9	82.1	1109.15	16.17	2.17	68.59
CuK	19.1	17.9	238.50	12.13	4.38	19.67
Total	100	100				

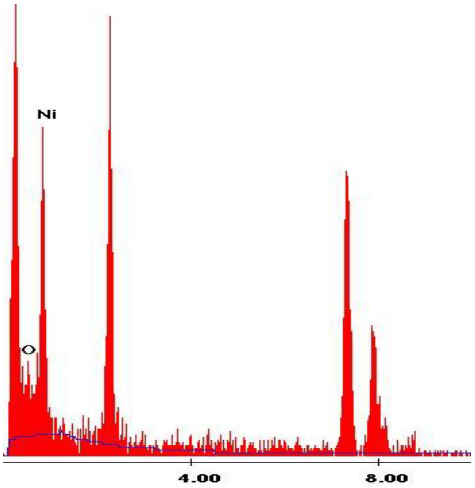

Element	Weight %	Atomic %	Net inte.	Backgrd.	Inte. error	P/B
OK	18.1	44.7	31.32	8.86	8.89	3.54
NiLK	81.9	55.3	126.56	11.39	3.84	11.11
Total	100	100				

Figure 7. EDX analysis of (a) nickel nanoparticles and (b) nickel oxide nanoparticles.

4.2. X-ray diffraction (XRD) analysis

X-ray diffractogram of the nickel and nickel oxide nanoparticles prepared are shown in figure 5 with the 2θ values lying between 30 and 80°. The XRD of the nanoparticles shows some broad and low intensity peaks. This is because the sample is mainly amorphous and/or also because the crystal domains are very small and less than 50 nm. We also observed peaks corresponding to face-centered cubic (fcc) nickel and nickel oxide. The XRD pattern of nickel nanoparticles, as in figure 5(a), shows two characteristic peaks at 2θ values of 44.7°, 52.6° corresponding to the marked indices of (111) and (200), respectively. These characteristic peaks indicate the formation of an fcc nickel phase without significant oxides or other impurity phases.

Figure 5(b) shows the XRD patterns for nickel oxide synthesized using hydrazine hydrate in air. The characteristic peaks occur at 2θ values of 37.60°, 43.65° and 63.20° corresponding to the marked indices of (111), (200) and (220), respectively. The average primary particle size of the nickel and nickel oxide nanoparticles was calculated from the full-width at half-maximum (FWHM) of the (111) peaks in the XRD patterns using the Scherrer equation. This results

in an average primary particle size of about 29 and 33 nm, respectively.

4.3. Selected area electron diffraction (SAED) analysis

Figure 6 shows the areas for the electron diffraction pattern of the resultant nanoparticles. We observed three main fringe patterns with their radii in the ratio of 0.20:1.75 Å which are close to the interplanar spacing values for Ni nanoparticles to the (111) and (200) planes. This could be because the resultant particles were purely metallic nickel with an fcc structure.

The corresponding electron diffraction pattern (figure 6(a)) shows sharp rings with plane distances of 2.99, 2.47, 2.12, 1.51, and 1.28 Å. This indicates the d-spacing for pure cubic nickel oxide. Figure 6(b) shows the electron diffraction pattern for nickel oxide nanoparticles. The spacing of 0.21 nm corresponds to the nickel oxide (200) planes and matches with the reported pattern shown by other research groups [34, 35].

4.4. Energy dispersive x-ray (EDX) analysis

The EDX was performed for the synthesized nickel and nickel oxide nanoparticles on various regions given in figures 7(a) and (b), respectively, and confirmed that the presence of respective nanoparticles as the elementary component with energy bands centered on 7.5 and 0.8 keV corresponds to K and L lines, respectively. Figure 7(b) shows the presence of oxygen with nickel as elementary components which confirm the formation of nickel oxide nanoparticles.

5. Catalytic activity

Nickel and nickel oxide nanoparticles synthesized by our protocol have been used by our group for catalyzing various chemical reactions such as the chemo-selective Knoevanagel condensation [12], synthesis of quinoxalines [1] and selective protection of carbonyl compounds [36]. These reactions show that the highly stable, monodispersed nanoparticles retain their catalytic activity up to five reaction cycles and are chemo-selective in nature. We have used our nanoparticles for synthesizing a number of different reactions [37–46].

6. Conclusions

The present study illustrates a novel, simple and convenient method for the synthesis of nickel and nickel oxide nanoparticles through the reduction of nickel salts in the water pool of reverse microemulsion. In the thermodynamically stable reverse microemulsion, nickel nanoparticles could be prepared by the reduction of $Ni(NO_3)_2$ with alkaline $NaBH_4$ and nickel oxide nanoparticles could be synthesized using hydrazine hydrate as a reducing agent. Nanoparticles formed were characterized using advanced sophisticated techniques such as QELS, TEM, XRD, electron diffraction and EDX which confirmed that particles formed were spherical in shape and pure. The size of the nanoparticles can be easily controlled by changing the molar ratio of water to surfactant or by altering the concentration of the reducing agent. The method illustrates a simple way of preparing nickel and nickel oxide nanoparticles.

Acknowledgments

The authors (SM, SA and AK) acknowledge the financial support from the Department of Science and Technology (DST), Council of Scientific Industrial Research (CSIR), and University Grant Commission (UGC), Government of India.

References

[1] Kumar A, Kumar S, Saxena A, De A and Mozumdar S 2008 *Catal. Commun.* **9** 778
[2] Knecht M R, Garcia-Martinez J C and Crooks R M 2006 *Chem. Mater.* **18** 5039
[3] Patel J D, Canar O and Jones J 2007 *Pharm. Res.* **24** 343
[4] Tan L H, Li F S and Liu L L 2003 *Mater. Rev.* **17** 41
[5] Chen R Y and Zhou K G 2006 *Trans. Nonferr. Met. Soc. China* **16** 1223
[6] Vladimir V B, Valentin N M and Nikolay V G 2005 *Chem. Vapor Depos.* **11** 368
[7] Qin Z P, Guo H X, Li D S and Shi X P 2004 *J. Funct. Mater. Dev.* **10** 95
[8] He Y Q, Li X G and Swihart M T 2005 *Chem. Mater.* **17** 1017
[9] Liu Z, Li S, Yang Y, Peng S, Hu Z and Qian Y 2003 *Adv. Mater.* **15** 1946
[10] Tang Z X, Sorensen C M, Klabunde K J and Hadjipanayis G C 1991 *J. Colloid Interface Sci.* **146** 38
[11] Fegley B J, White P and Bowen H K 1985 *Am. Ceram. Soc. Bull.* **64** 1115
[12] Kumar A, Dewan M, Saxena A, De A and Mozumdar S 2010 *Catal. Commun.* **11** 679
[13] Gao B J, Gao J F, Zhou J Q and Chin J 2001 *Inorg. Chem.* **17** 491
[14] Chen D H and Wu S H 2000 *Chem. Mater.* **12** 1354
[15] Hou Y and Gao S 2003 *J. Mater. Chem.* **13** 1510
[16] Green M and O'Brien P 2001 *Chem. Commun.* **19** 1912
[17] Chen D H and Hsieh C H 2002 *J. Mater. Chem.* **12** 2412
[18] Chen L, Chen J, Zhou H, Zhang D and Wan H 2007 *Mater. Sci. Eng.* A **262** 452
[19] Jeon Y T, Moon J Y, Lee G H, Park J and Chang Y 2006 *J. Phys. Chem.* B **110** 1187
[20] Jeon Y, Lee G H, Park J, Kim B and Chang Y 2005 *J. Phys. Chem.* B **109** 12257
[21] Murray C B, Sun S, Doyle H and Betley T 2001 *MRS Bull.* **26** 985
[22] Toneguzzo P, Viau G, Acher O, Guillet F, Bruneton E and Fievet V F 2000 *J. Mater. Sci.* **35** 3767
[23] Hinotsu T, Jeyadevan B, Chinnasamy C N, Shinoda K and Tohji K 2004 *J. Appl. Phys.* **95** 7477
[24] Chinnasamy C N, Jeyadevan B, Shinoda K, Tohji K, Narayanasamy A, Sato K and Hisano S 2005 *J. Appl. Phys.* **97** 10J309
[25] Tzitzios V, Basina G, Gjoka M, Alexandrakis V, Georgakilas V, Niarchos D, Boukos N and Petridis D 2006 *Nanotechnology* **17** 3750
[26] Park J W, Chae E H, Kim S H, Lee J H, Kim J W and Yoon S M 2006 *Mater. Chem. Phys.* **97** 371
[27] Goh C F, Yu H, Yong S S, Mhaisalkar S G, Boey F Y C and Teo P S 2005 *Mater. Sci. Eng.* B **117** 153
[28] Jiang C, Zou G, Zhang W, Yu W and Qian Y 2006 *Mater. Lett.* **60** 2319
[29] Luisi P L and Magid L J 1986 *Crit. Rev. Biochem.* **20** 409
[30] Pileni M P (ed) 1989 *Structure and Reactivity in Reverse Micelles* (Amsterdam: Elsevier)
[31] Paul B K and Moulik S P J 1997 *Dispers. Sci. Technol.* **18** 301

[32] La M V K and Dinegar R H 1950 *J. Am. Chem. Soc.* **72** 4847
[33] Liu Q, Liu H J, Liang Y Y, Xu Z and Yin G 2006 *Mater. Res. Bull.* **41** 697
[34] Phung X, Groza J, Stach E A, Williams L N and Ritchey S B 2003 *Mater. Eng.* A **359** 261
[35] Chen Y, Peng D L, Lin D and Luo X 2007 *Nanotechnology* **18** 505703
[36] Kumar A, Kumar S, Saxena A, De A and Mozumdar S 2008 *Catal. Lett.* **122** 98
[37] Kumar A, Aerry S, Saxena A, De A and Mozumdar S 2012 *Green Chem.* **14** 1298
[38] Dewan M, Kumar A, Saxena A, De A and Mozumdar S 2012 *PLoS ONE* **7** e29131
[39] Dewan M, Kumar A, Saxena A, De A and Mozumdar S 2010 *Tet. Lett.* **51** 6108
[40] Dewan M, Kumar A, Saxena A, De A and Mozumdar S 2012 *PLoS ONE* **7** e43078
[41] Kumar A, Dewan M, Saxena A, De A and Mozumdar S 2011 *Tet. Lett.* **52** 4835
[42] Kumar A, Singh P, Saxena A, De A and Mozumdar S 2008 *Catal. Commun.* **10** 17
[43] Kumar A, Dewan M, Saxena A, De A and Mozumdar S 2013 *RSC Adv.* **3** 603
[44] Aerry S, De A, Kumar A, Saxena A, Majumdar D K and Mozumdar S 2012 *J. Biomed. Mater. Res.* A doi: 10.1002/jbm.a.34476
[45] Aerry S, Kumar A, Saxena A, De A and Mozumdar S 2013 *Green Chem. Lett. Rev.* **6** 183–8
[46] Kumar A, Saxena A, De A, Shankar R and Mozumdar S 2013 *RSC Adv.* **15** 5015–21